Optik 126 (2015) 3276–3282

Contents lists available at ScienceDirect

Optik

journal homepage: www.elsevier.de/ijleo

Fast contour torque features based recognition in laser active imaging system

Canjin Wang[a,b,*], Tao Sun[a], Tinfeng Wang[a], Juan Chen[a]

[a] State Key Laboratory of Laser Interaction with Matter, Changchun Institute of Optics, Fine Mechanics and Physics, Chinese Academy of Science, Changchun, Jilin, China
[b] University of Chinese Academy of Sciences, Beijing, China

ARTICLE INFO

Article history:
Received 15 July 2014
Accepted 3 August 2015

Keywords:
Laser active imaging
Recognition
Contour torque
Affine invariant
Feature regions

ABSTRACT

Recent years laser active imaging system are widely used as a useful detection artifice. While many denoising and enhancing algorithms have been proposed, target recognition in laser active imaging is still a new domain that few researches have been done. Classical recognition methods often break done due to the characteristic of laser active imaging. In this paper we present a novel target recognition method based on fast contour torque features (FCTF). The proposed fast contour torque features contain abundant information of the target, such as the size, position, darkness and shape regularly of the contours. Meanwhile the features are invariant to rotation, scaling and affine transform, and can be computed efficiently.

We first extract feature regions by MSER algorithm, and transform them into circular areas, so the regions are invariant to affine transform. Then local invariant features of the feature regions were extracted by fast contour torque feature descriptor and we input into the trained SVM classifier for identify. Comprehensive experiments show that our approach achieves higher recognition rate in rotation and affine transformation as state-of-art method, and meet the real-time requirement in laser active imaging.

© 2015 Elsevier GmbH. All rights reserved.

1. Introduction

Laser active imaging is a new detection method which performs better than the passive imaging system under conditions of poor visibility due to laser's high intensity and high collimation [1,2]. With laser active imaging systems, it is possible to classify and identify targets of interest at night, which has broad application prospects in the military, civilian security and other fields [3–5]. Nowadays researches on target recognition for laser active imaging system is still in its infancy at home and aboard and few can learn from literature. Due to the difference of imaging mechanism and imaging conditions, with respect to the target recognition under visible passive imaging, active laser illumination target recognition has the following characteristics:

(1) An inherent noise – speckle noise is introduce by laser's coherence, thus blurring the image details;
(2) CCD noise and noise caused by atmospheric transport decrease image contrast, seriously affecting the image quality;
(3) Uneven illumination in target's different areas increases the difficulty of target segmentation;
(4) When the laser power is changed, the gray level and contrast of target and the background are changed;
(5) Due to laser's monochromatic, the color characteristics of the target are difficult to obtain;
(6) Real-time requirement for the system needs to complete the identification process within a single frame time.

These characteristics above make most identification methods based on gray, texture and color are difficult to apply in the laser active imaging target recognition system, which increases the difficulty of identification.

For the features of laser active imaging, we proposed a recognition method based on fast contour torque features (FCTF). The features are invariant to rotation, scale and affine transform, with which we could real-time, accurately identify the target. The proposed method comprises three steps: first, detect the target's feature regions with MSER and transform them into circular areas; second, calculate FCTF for each feature areas; third, input the FCTFs into trained SVM for recognition.

* Corresponding author at: State Key Laboratory of Laser Interaction with Matter, Changchun Institute of Optics, Fine Mechanics and Physics, Chinese Academy of Science, Changchun, Jilin, China. Tel.: +86 05973622339.
E-mail address: wcjpsh@126.com (C. Wang).

http://dx.doi.org/10.1016/j.ijleo.2015.08.014
0030-4026/© 2015 Elsevier GmbH. All rights reserved.

2. Related work

Relative to grayscale and color information, the contour of the target is easier to extract in laser active imaging. Contour features provide information about the target's shape and play an important role in target recognition. Currently recognition methods based on contour features include: Belongie [6] proposed shape context feature descriptor, in which contour points distribution histogram were added up in polar coordinates. When discontinuity occurs in the contours, the targets can still be identified. Jurie et al. [7] proposed a scale-invariant feature detection algorithm. They regarded the extreme region of the edge energy and entropy as a significant area of the region, then used the space distribution of the annular neighborhood points in the region to construct feature vectors. Fergus et al. [8] segmented contour and boundary by double tangency points, and tested their methods by identifying the constellation model. To identify shape-changed objects in video sequences, Kumar [9] proposed a Bayesian model graph structure. Shotton et al. [10] proposed to randomly sample rectangle from the training picture and generate contour fragments detection operator. Opelt [11] outlines principles to find fragments from the fragments pool based on the principle that the occurrence probabilities of the positive examples are the maximum and that of the negative examples are minimum. Zhu [12] proposed a technique for grouping the contour and segmented the contours in different scales. The algorithms above contain complex calculations and do not take into account complex motion of the target. When objects perform affine transformation, these algorithms may fail. Therefore, they are not applicable to occasions that have high demands on real-time and recognition accuracy, such as laser active imaging.

3. Extracting feature areas

Moving targets often perform rotation, scaling, illumination changes and affine transformation. In order to recognize targets accurately, we hope the extracted features are also invariant to the transformation above.

3.1. Maximally stable extremal regions

Lots of researches have been done on affine invariant region extraction methods: Lindeberg [13] proposed a shape adaptive smoothing algorithm, which estimated affine invariant regions in scale space using second moment matrix iteratively. Baumberg et al. [14] first sought Harris corners in scale space, and use them as the centers to iteratively estimate affine invariant regions. Tuytelaars et al. [15] improved Baumberg's method, they constructed affine invariant regions by locating edge points around Harris corners. These regions were more stable. Matas [16] proposed MSER (maximally stable extremal regions). The regions separated by different thresholds were merged and the most stable areas were defined as MSER. Mikolajczyk [17] promoted two kinds of famous feature points to affine invariant regions, which were known as Harris-affine and Hessian-affine. Mikolajczyk [18] then compared the performance of different affine invariant region detectors in viewpoint changes, scale changes and image compression, and concludes that MSER has the highest repetition rate, especially for homogeneous regions. In laser active imaging, the target is generally homogeneous and with high contrast, so we use MSER into laser active imaging recognition.

Let $S = \{0, 1, \ldots, 255\}$, a grayscale image $I : D \subset Z^2 \to S, A \subset D$ is the four-neighbor connection relationship, Q is a sub-region of D, if for any pixel p, $q \in Q$,

$$pAa_1, a_1pa_2, \ldots, a_nAq \tag{1}$$

where $a_i \in Q$, $i = 1, \ldots, n$, then we call Q an extremal region.

Let ∂Q be the boundary of Q, the pixels in ∂Q do not belong to Q, but are adjacent to at least one of pixels in Q.

$$\partial Q = \left\{ q | q \in D - Q, \exists p \in Q, qAp \right\} \tag{2}$$

where p is one of pixels in Q.

For any $p \in Q$, $q \in \partial Q$, if $I(p) > I(q)$, we call Q the maxima region, if $I(p) < I(q)$, we call Q the minimum region.

For nested extreme regions get by different threshold $\{Q_1, Q_2, \ldots, Q_i, \ldots\}$, let

$$q(i) = \frac{|Q_{i+\Delta} - Q_{i-\Delta}|}{|Q_i|} \tag{3}$$

where $|\bullet|$ means the number of regions, Δ is the threshold width. If $q(i^*)$ is the local minima of $q(i)$, we call Q_{i^*} the maximally stable extremal regions.

Let the threshold change from 0 to 255 and segment the image, with formula (3) we can get the positive maximally stable extremal regions MSER_+. The reverse the image and segment it we can get the negative maximally stable extremal regions MSER_-. The whole $\text{MSER} = \text{MSER}_+ \cup \text{MSER}_-$. In order to speed up the computation, we sorted the pixels first by box sorting method, of which computational complexity is $O(n)$. The we extracted and restored the consequent regions by the structure of spanning tree. After the optimization above the computational complexity of MSER is O (nloglogn).

3.2. Ellipse fitting and region conversion

The feature regions extracted by MSER are of any shapes. On the one hand, the boundary of MSER is not included in the feature region, which does not facilitate the extraction of the contour feature. On the other hand, the invariant feature of an arbitrary shape is difficult to construct. So we fitted the MSER regions to regular circular regions.

Let Σ be the covariance matrix of Q, which is

$$\Sigma = \begin{bmatrix} M_{20} & M_{11} \\ M_{11} & M_{02} \end{bmatrix} \tag{4}$$

where

$$M_{20} = \frac{1}{M_{00}} \sum \sum_{Q} (x - x_u)^2 I(x, y) \tag{3}$$

$$M_{11} = \frac{1}{M_{00}} \sum \sum_{Q} (x - x_u)(y - y_u) I(x, y) \tag{5}$$

$$M_{02} = \frac{1}{M_{00}} \sum \sum_{Q} (y - y_u)^2 I(x, y) \tag{6}$$

$$M_{00} = \sum \sum_{Q} I(x, y) \tag{7}$$

$$x_u = \frac{1}{M_{00}} \sum \sum_{Q} x I(x, y) \tag{8}$$

$$y_u = \frac{1}{M_{00}} \sum \sum_{Q} y I(x, y) \tag{9}$$

A matrix A maps the unit circle centered at $P_u(x_u, y_u)$ to a ellipse, which is

$$[A(X - P_u)]^T \Sigma^{-1} [A(X - X_u)] = 1 \tag{10}$$

where

$$(X - P_u)^T (X - X_u) = 1 \tag{11}$$

According to formulae (10) and (11), we get

$$A^T \Sigma^{-1} A = I \tag{12}$$

Then according to formulae (4) and (12), we get

$$A = \frac{1}{\sqrt{M_{02}}} \begin{bmatrix} \sqrt{M_{20}M_{02} - M_{11}^2} & M_{11} \\ 0 & M_{02} \end{bmatrix} \tag{13}$$

With the transform matrix A above, we can transform any feature region Q to elliptical area. The parameters of the ellipse are determined by Eq. (13).

Then the elliptical area should be mapped to circular area, so is invariant to translating, scaling and affining. Let B be the transformation matrix:

$$\left[B(X - P_u)^T\right] \left[B(X - P_u)\right] = r^2 \tag{14}$$

where r is the radius. Also we can describe the points on the ellipse as

$$(X - P_u)^T \Sigma^{-1} (X - P_u) = 1 \tag{15}$$

According to formulae (15) and (16), we get

$$B = \frac{r}{\sqrt{M_{20}\left(M_{20}M_{02} - M_{11}^2\right)}} \begin{bmatrix} \sqrt{M_{20}M_{02} - M_{11}^2} & 0 \\ -M_{11} & M_{20} \end{bmatrix} \tag{16}$$

In summary, with the transformation matrix A and B, the feature region of any shape can be converted to a circular region, of which the center is the centroid of the original feature region, and the radius of the circular region is adjustable. After transformation, the circular area is invariant to rotating, scaling, and affining.

4. Features based on contour torque

4.1. Contour torque

Assuming c is the contour of a sub-region, we define the force of any pixel p in c as

$$\vec{f}(p) = \frac{\nabla I(p)^{\perp}}{|\nabla I(p)|} \tag{17}$$

where $\nabla I(p) = (I_x, I_y)$ denotes the gradient of p. $\nabla I(p)^{\perp}$ is perpendicular to $\nabla I(p)$ and points to counterclockwise. Due to formula (17), the force $\vec{f}(p)$ discards the gradient magnitude information and weakens the influence of different contrast to target recognition.

For any patch P_a, let o denote the center of P_a, p denote any point of P_a, the torque of p is defined as

$$\rightarrow t(p) = \rightarrow op \times \rightarrow f(p) \tag{18}$$

where $\rightarrow op$ is a vector from contour center to p, $\times$ is vector cross multiplication.

The force $\vec{f}(p)$ and torque $\vec{t}(p)$ of p are shown in Fig. 1.

Let $\tau_o(p)$ denote the norm of $\vec{t}(p)$, $\tau_o(p)$ can be calculated as

$$\tau_o(p) = |\vec{op}||\vec{f}(p)| \sin\theta = op \sin\theta \tag{19}$$

where $\theta \in [0^o, 360^o)$ denotes the angle between $\vec{f}(p)$ and $\vec{op}$.

From (19) we can conclude that contour torque depicts the trend of contour curvature and for a closed contour, the set of contour torque can uniquely describe the contour.

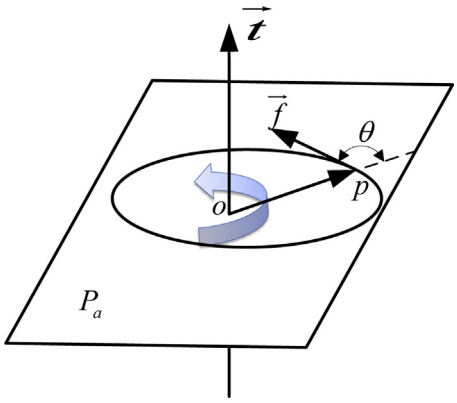

Fig. 1. The force and torque defined in (17) and (18). o denotes the center and θ denote the angle between $\rightarrow op$ and $\vec{f}(p)$.

For any image patch P_a, we define its contour torque as

$$\Gamma_o = \sum_{i=1}^{n} \tau_o(p_i) \tag{20}$$

where n denotes the point number.

The more regular the contour is, the larger Γ_o calculated from (20). Meanwhile Γ_o describes the size and position of the contours within the patch: larger Γ_o means the contour is close to the patch boundries. The Γ_o of convex contour is larger than that of concave contour. According to the definition of the edge direction, contour torque of light target on dark background is greater than 0, and contour torque of dark target on light background is less than 0.

Totally, the contour torque features can represent the size, position, regularity and lightness of the contour in image patch. In the case of image patches having a unique closed contour, with contour torque features can restore the contour. In this case, we can use contour torque features in target recognition.

4.2. Contour features based on torque

In this section we intend to design a local invariant feature based on contour torque, then use it into target recognition.

Contour torque abandons gradient information of the patches, so it is robust to illustration changes. From (20) we can easily conclude that it is invariant to rotation. In order to ensure scaling invariant characteristic, we normalize (20) as

$$\hat{\Gamma}_o = \frac{\Gamma_o}{r^2} = \frac{\sum_{i=1}^{n} \tau_o(p_i)}{r^2} \tag{21}$$

where r is the radius of the regular circular region. Since n, $\tau_o(p_i)$, r is linear with image scale, $\hat{\Gamma}_o$ is invariant to scaling.

To every regular circular feature region Q, we construct Fast Contour Torque Features (FCTF) shown as Fig. 2.

(1) Eight sampling points $\{O_1, O_2, \ldots, O_8\}$ distributed on the circle centered in O and with a radius of $r/2$. In order to ensure the sampling points are rotational invariance, OO_1 points to the main direction calculated similar to SURF: pick fan-shaped areas in the circle with a angle of 60° and calculate their $\hat{\Gamma}$. After traversing the circular feature region, we take the direction of the fan-shaped area with maximum $\hat{\Gamma}$ as the main direction of the circular feature region.
(2) According to formula (22), calculate the normalized contour torque features $\hat{\Gamma}_{o_1}, \hat{\Gamma}_{o_2}, \ldots, \hat{\Gamma}_{o_8}$ of the circles centered in $\{O_1, O_2, \ldots, O_8\}$ and with a radius of $r/4$.

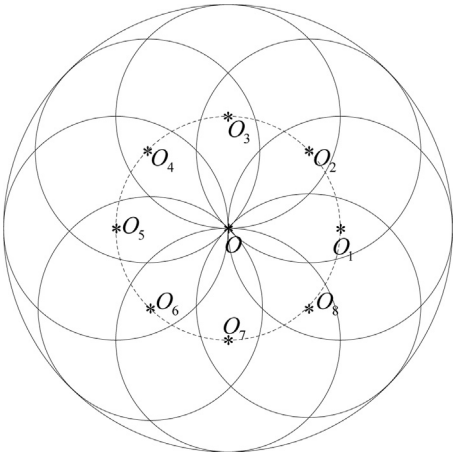

Fig. 2. Sample pattern of FCTF.

(3) Calculate the normalized contour torque feature $\hat{\Gamma}_o$ of the circle centered in O and with a radius of r.
(4) Integrate the results of Step (2) and (3) we can get the final as follows: $\mathrm{FCTF}(O, r) = \{\hat{\Gamma}_o, \hat{\Gamma}_{o_1}, \hat{\Gamma}_{o_2}, \ldots, \hat{\Gamma}_{o_8}\}$.

From the definition of FCTF we can conclude that its computation mainly focuses on two parts: determining the main direction and calculating the contour torque feature of each sampling area. Both need a large amount of calculation of contour torque. In order to improve computational efficiency, contour torque can be calculated using a speed-up method. Assuming the upper left corner of the whole image as the origin o_r, for a image patch Q centered in o, its contour torque can be calculated as

$$\begin{aligned}\vec{T}_o(Q) &= \sum_{p\in Q} \vec{op} \times \vec{f}(p) \\ &= \sum_{p\in Q} \left(\vec{oo_r} + \vec{o_r p}\right) \times \vec{f}(p) \\ &= \vec{oo_r} \times \sum_{p\in Q} \vec{f}(p) + \sum_{p\in Q} \vec{o_r p} \times \vec{f}(p)\end{aligned} \tag{22}$$

Whenever an image is read, $\vec{f}(p)$ and $\vec{o_r p} \times \vec{f}(p)$ for its each pixel p can be precalculated and restored into a table. Then for any patch Q in the image, its contour torque $\vec{T}_o(Q)$ can be calculated within one multiplication and a few simple addition. This greatly speeds up the computation of FCTF and satisfies the real-time requirement of laser active recognition system.

5. Target recognition based on fast contour torque features (FCTF)

The basic procedure of the proposed recognition method for laser active imaging system based on fast contour torque features is as follows:

Step 1 Extract affine invariant feature regions using MSER, and fit them into circular regions.
Step 2 For each circular region, extract its FCTF
Step 2 For a set of training images, repeat Step 1 and Step 2, input the positive and negative FCTFs into SVM [19] for training
Step 4 In the recognition stage, for each input image, repeat Step 1 and Step 2 and input its FCTFs into the trained SVM for identification.

Fig. 3. Laser active imaging and recognition system.

6. Experiments

6.1. System and imaging results

We ran comprehensive experiments for evaluating our approaches. We first constructed a laser active imaging system shown as Fig. 3: The laser emission system was a near-infrared fiber-coupled semiconductor laser with the wavelength of 793 nm, power of 3W and divergence angle of 5 mrad. The optical imaging system was Falcon HG 1M120CMOS camera with resolution of 1024×1024 and pixel size of 7.4 μm. The control turntable was YS3081 two-turntable bearing carrier with size of $341 \times 206 \times 390$ mm, weight of 20 kg, azimuth of 0–360° and elevation of −45–45°. The imaging system was connected with a frame grabber on the IPC via cameralink interface. The laser emission system transmitted infrared laser to irradiate target area in distance. The light signal is reflected back to the optical imaging system by the objective and the imaging system transmitted images to the IPC in a frame rate of 25 fps. Finally we recognize the target using the proposed algorithm. The configuration of IPC was: i7-2600 3.40 GHz CPU, 4 GB RAM.

A pure black model gun with a size of 80 cm × 24 cm × 4 cm was used as the target and put in the distance of 450 m and 550 m far to the imaging system at night. The imaging results are shown in Fig. 4. From the images we can see that although good contrast was there between target and background, speckle noise is so serious that increased the difficulty of identifying. Farther away from the target, the more severely the laser diffused and attenuated, and the weaker reflected light the system received. So we noticed that the illumination in 550 m was weaker than that in 450, and visually the target was more fuzzy.

6.2. Extracting affine invariant regions

We used MSER to extract the interesting elliptic regions and eliminated regions that were obviously too small, the result was shown in Fig. 5(a). We can see that the algorithm could extract the complete target area. Set $r = 45$ and regularized the elliptical areas, the results were shown in Fig. 5(b). After regularization, the target shape within circular areas is basically the same. Especially when the target performed affine transformation, the shape was seriously distorted, while after the regularization, the shape was largely corrected. So we can get the conclusion that the selected feature region extracted method was invariant to rotation and affining.

6.3. Training SVM

After extracting the regularized circular regions, we search the edge fragments them using Canny operator, then computed the

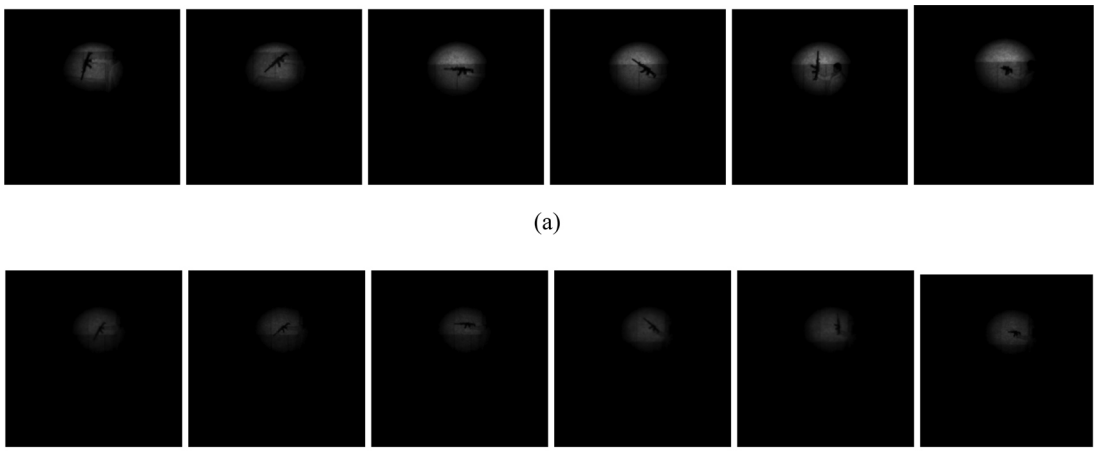

Fig. 4. Active imaging result in different distance. (a) Active imaging result in 450 m, (b) active imaging result in 550 m.

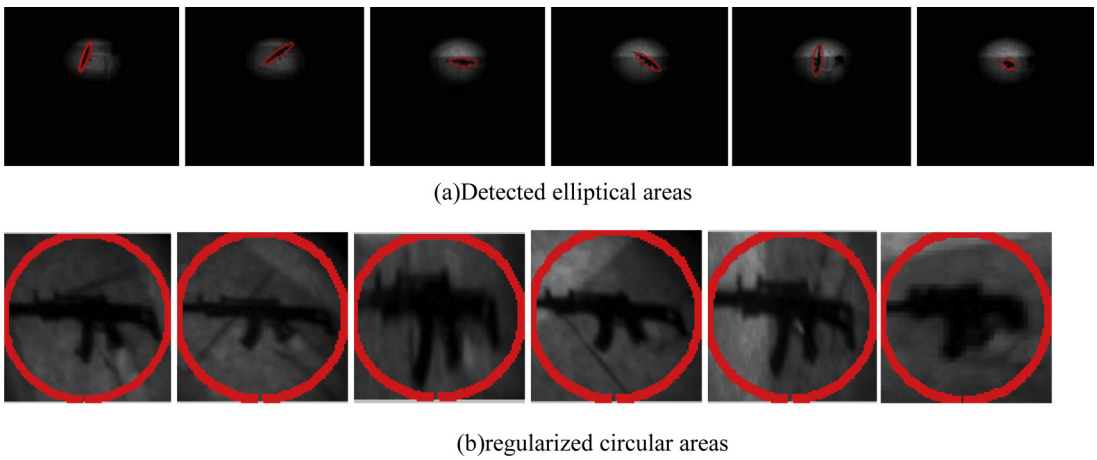

Fig. 5. Feature region detection result by MSER. (a) Detected elliptical areas, (b) regularized circular areas.

FCTFs and input into SVM for training. We use 500 gun images as positive training samples and 500 other images as negative samples. Some of the positive and negative samples are shown in Fig. 6(a) and (b), respectively.

6.4. Recognition results

For every image from laser active imaging system, first extracted its circular feature region, than computed FCTFs and input into the

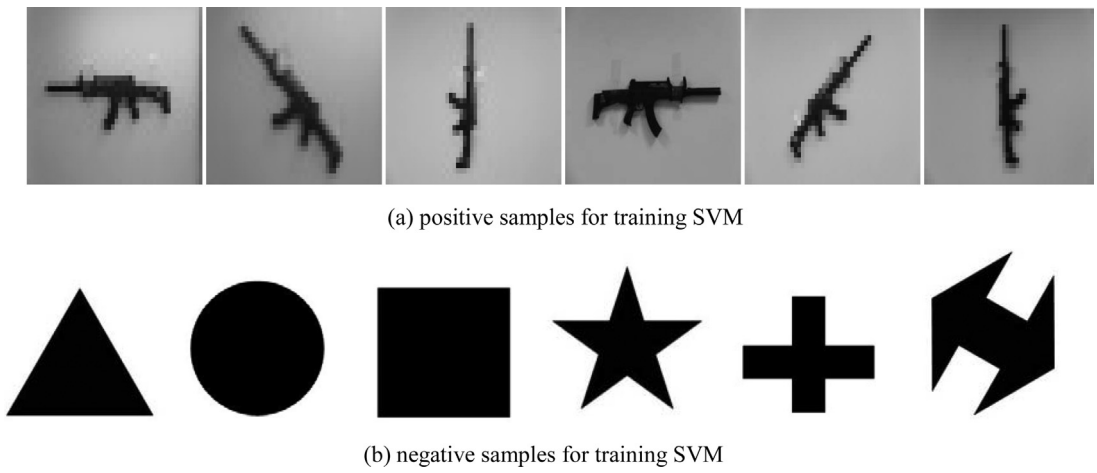

Fig. 6. Positive and negative pictures for SVM training. (a) Positive samples for training SVM, (b) negative samples for training SVM.

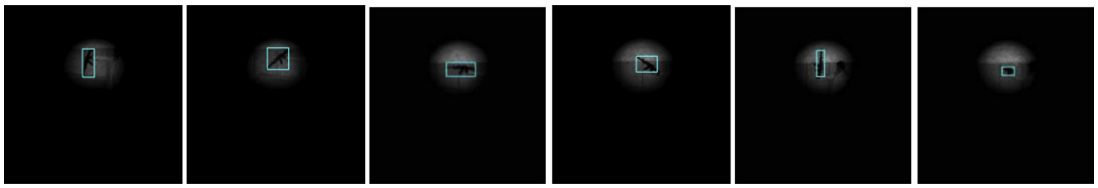

Fig. 7. Recognition results of rob at 450 m from experiment platform at night.

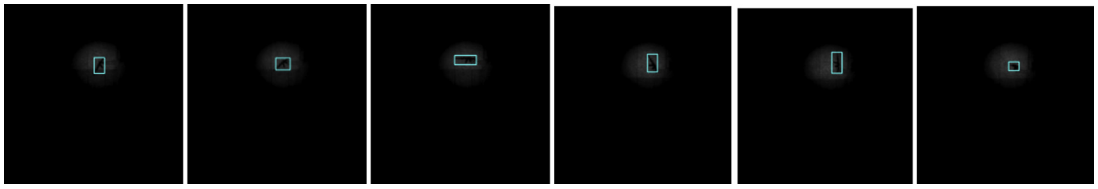

Fig. 8. Recognition results of rob at 550 m from experiment platform at night.

Table 1
Statistics of recognition rate at 450 m and 550 m at night.

Target distance (m)	Target transform	Recognition rate by *k*AS + BoF	Recognition rate by Boiman shape + BoF	Recognition rate by proposed method
450	Rotation	**85.72**	65.29	84.46
	Affine	54.36	44.17	**68.39**
	Rotation + affine	67.27	67.38	**83.25**
550	Rotation	83.57	62.34	**85.19**
	Affine	47.14	46.53	**67.36**
	Rotation + affine	70.18	53.63	**74.20**

trained SVM for identification. We performed the experiments at night in distance of 450 m and 550 m, and the target moved as Fig. 7 shows (rotation and affine transform). The recognition results are shown in Figs. 7 and 8, respectively. We can see that when the target performed rotation and affine transform, our algorithm could still recognize accurately.

We compare our method with state-of-the-art laser active imaging recognition methods proposed in [20] (denoted as *k*AS + BoF) and [21] (denoted as Boiman Shape + BoF), in both recognition rate and speed. For *k*AS, we used $k = 1,2,3,4$, which meant that there were 4 types of descriptors in one region. For Bioman Shape, we set the dim of the descriptor as 192. The recognition rates of different methods are reported in Table 1. As can be seen, in most scenes our approach outperformed the other two methods, especially in affine and rotation + affine transform. This is not surprising, since *k*AS are not affine invariant, and Boiman Shape descriptor are sensitive to speckle noise. For all the three approaches, the recognition rate of rotation is much higher than that of affine and rotation + affine, since affine transform would change the shape severely.

In most cases, the recognition rate in 550 m is lower than that in 450 m, which is understandable. In 550 m, the spot energy is diffused more severely than in 450 m, while the contrast between target and background is lower. Also the speckle noise is higher, which makes features extraction more difficult.

Table 2 shows the processing speed using three methods above. We can see that the proposed method is much faster than the other two, which proved the efficiency of our accelerated method. While the system operating in a frame rate of 25 fps, only our proposed method can satisfy the requirement of real-time processing of the system.

Table 2
Statistic of cost time in single frame for different methods.

	Cost time (ms)
*k*AS + BoF	77.46
Boiman shape + BoF	52.05
proposed method	**23.68**

7. Conclusion

We have presented a target recognition method suitable for laser active imaging system based fast contour torque feature (FCTF). We have discussed the difficulties in laser active imaging, and got the conclusion that contour features were suitable for recognition. In this case, we extended the concept of torque into image processing and the proposed FCTF is invariant to rotation and affine transform. We evaluated the scheme on laser active system and the experimental results indicated that our approach outperformed other state-of-the-art recognition methods while satisfying the requirement of real-time processing.

Acknowledgements

This research is supported by Science and Technology Development Program of Jilin, China (Grant no. 20126015). The authors would like to thank the reviewers for their valuable comments and suggestions that improve the presentation of this paper.

References

[1] K. Sugioka, Y. Cheng, Ultrafast lasers – reliable tools for advanced materials processing, Light: Sci. Appl. 3 (4) (2014) e149.
[2] D. Wu, J. Xu, L.G. Niu, et al., In-channel integration of designable microoptical devices using flat scaffold-supported femtosecond-laser microfabrication for coupling-free optofluidic cell counting, Light: Sci. Appl. 4 (1) (2015) e228.
[3] M. Laurenzis, F. Christnacher, D. Monnin, Long-range three-dimensional active imaging with superresolution depth mapping, Opt. Lett. 32 (21) (2007) 3146–3148.
[4] C. Vannahme, M. Dufva, A. Kristensen, High frame rate multi-resonance imaging refractometry with distributed feedback dye laser sensor, Light: Sci. Appl. 4 (4) (2015) e269.

[5] C.J. Wang, T. Sun, N.N. Shi, et al., Laser active imaging and recognition system based on double hidden layer BP algorithm, Opt. Precis. Eng. 22 (6) (2014) 1639–1647.
[6] G. Mori, S. Belongie, J. Malik, Efficient shape matching using shape contexts, IEEE Trans. Pattern Anal. Mach. Intell. 27 (11) (2005) 1832–1837.
[7] F. Jurie, C. Schmid, Scale-invariant shape features for recognition of object categories, in: IEEE Computer Society Conference on Computer Vision and Pattern Recognition (CVPR 2004), 2004, pp. II-90–II-96, vol. 2.
[8] R. Fergus, P. Perona, A. Zisserman, A visual category filter for Google images, in: Computer Vision-ECCV 2004, Springer, Berlin, Heidelberg, 2004, pp. 242–256.
[9] M.P. Kumar, P.H.S. Torr, A. Zisserman, Extending pictorial structures for object recognition, in: Proc. BMVC, 2004, pp. 81.1–81.10.
[10] J. Shotton, A. Blake, R. Cipolla, Contour-based learning for object detection, in: IEEE Tenth International Conference on Computer Vision (ICCV 2005), 2005, pp. 503–510, vol. 1.
[11] A. Opelt, A. Pinz, A. Zisserman, A boundary-fragment-model for object detection, in: Computer Vision–ECCV 2006, Springer, Berlin, Heidelberg, 2006, pp. 575–588.
[12] Q. Zhu, L. Wang, Y. Wu, et al., Contour context selection for object detection: a set-to-set contour matching approach, in: Computer Vision–ECCV 2008, Springer, Berlin, Heidelberg, 2008, pp. 774–787.
[13] T. Lindeberg, J. Gårding, Shape-adapted smoothing in estimation of 3-D shape cues from affine deformations of local 2-D brightness structure, Image Vision Comput. 15 (6) (1997) 415–434.
[14] A. Baumberg, Reliable feature matching across widely separated views, in: Processings of Conference on Computer Vision and Pattern Recognition, Hilton Head Island, SC, USA, 2000, pp. 774–781.
[15] T. Tuytelaars, L. Van Gool, Content-based image retrieval based on local affinely invariant regions, in: Visual Information and Information Systems, Springer, Berlin, Heidelberg, 1999, pp. 493–500.
[16] J. Matas, O. Chum, M. Urban, et al., Robust wide-baseline stereo from maximally stable extremal regions, Image Vision Comput. 22 (10) (2004) 761–767.
[17] K. Mikolajczyk, C. Schmid, Scale & affine invariant interest point detectors, Int. J. Comput. Vis. 60 (1) (2004) 63–86.
[18] K. Mikolajczyk, T. Tuytelaars, C. Schmid, et al., A comparison of affine region detectors, Int. J. Comput. Vis. 65 (1–2) (2005) 43–72.
[19] J. Li, L.H. Guo, Target threat assessment using improved SVM, Opt. Precis. Eng. 22 (5) (2014) 1354–1362.
[20] V. Ferrari, L. Fevrier, F. Jurie, et al., Groups of adjacent contour segments for object detection, IEEE Trans. Pattern Anal. Mach. Intell. 30 (1) (2008) 36–51.
[21] O. Boiman, E. Shechtman, M. Irani, In defense of nearest-neighbor based image classification, in: IEEE Conference on Computer Vision and Pattern Recognition (CVPR 2008), 2008, pp. 1–8.